Rev. Mexicana Astron. Astrof., 11, 149-157 (1985)

OPTICAL IMAGES OF THE REGION AROUND HH1 AND HH2 TAKEN WITH THE MEPSICRON SYSTEM

J. Bohigas, J.M. Torrelles[1], J. Echevarría, J. Cantó, R. Enríquez, C. Firmani, L. Gutiérrez, E. Ruiz, and L. Salas

Instituto de Astronomía
Universidad Nacional Autónoma de México

Received 1985 August 5

RESUMEN

Utilizando el sistema de detección *MEPSICRON*, obtuvimos imágenes directas de la región que contiene a los objetos Herbig-Haro 1 y 2. Estas imágenes fueron tomadas con filtros de interferencia centrados en Hα, en el continuo rojo (6648 A) y en la línea del [S II] en 6731 A. Encontramos dos nebulosas cónicas que unen la fuente central de continuo en radio con los objetos HH1 y HH2. Las líneas de emisión (Hα y [S II]) son producidas localmente, y probablemente excitadas por una onda de choque generada por el viento estelar que surge de la fuente central. La emisión de continuo es reflexión de luz posiblemente producida por la misma fuente. A unos 10″ al NE de la fuente central detectamos una pequeña nebulosa con una fuerte emisión en las líneas de azufre. Asimismo, encontramos un par de condensaciones de emisión a ~ 20″ W de la misma fuente. El cociente de azufre entre Hα sugiere que la nebulosa y estas dos condensaciones están siendo ionizadas colisionalmente. Finalmente, no detectamos emisión proveniente de la fuente central de continuo en radio. Debido a esto, estimamos que esta fuente debe ser más débil que $m_V \sim 21.5$

ABSTRACT

Using the *MEPSICRON* detection system, we obtained images of the region around Herbig-Haro objects 1 and 2. These images were taken with interference filters centered at Hα, at the red continuum (6648 A) and at the [S II] line at 6731 A. We found two conical nebulosities uniting the central radio continuum source with HH1 and HH2. The emission lines (Hα and [S II]) are produced *in situ*, being probably excited by a shock wave created by the stellar wind emerging from the central source. Continuum emission is likely reflected light from the same source. Some 10″ to the NE of the central source we detected a small nebulosity with strong sulphur emission. Similarly, two emission knots were found ~ 20″ W of this source. The sulphur to hydrogen ratio indicates that the nebulosity and the two knots are collisionally ionized. Finally, we did not detect optical emission from the central radio continuum source. This implies a limiting visual magnitude of 21.5 for this source.

Key words: **STAR-FORMING REGIONS — NEBULAE – INDIVIDUAL — HERBIG – HARO OBJECTS**

I. INTRODUCTION

Herbig-Haro (HH) objects have been the subject of intensive research since they were discovered (Haro 1950, 1952; Herbig 1951). After a long controversy, it is now firmly established that these objects are the cooling region of a gas that has been collisionally excited by a shock wave, which is probably produced by a stellar wind (a review on the principal characteristics of HH objects can be found in Cantó 1981 and Schwartz 1983).

The prototype of this class of celestial entities are HH1 and HH2, which are located 2° to the SE of the Orion Nebula. Each of the HH1 and HH2 objects is constituted by a number of knots. Research on the proper motions of these knots (Herbig and Jones 1981) indicates that HH1 and HH2 are moving in opposite directions, with tangential velocities close to 300 km s^{-1} along the line connecting them. These velocities are much larger than the observed radial velocities, which are about 10 km s^{-1}, implying a spatial motion nearly perpendicular to the line of sight. Such a motion has been interpreted as due to the action of a collimated bipolar wind produced by a stellar source lying near the line connecting the two HH objects. The location of the exciting source, in the HH1-2 region as well as in other systems with Herbig-Haro objects, is one of the more important questions to be solved if we are to understand the origin of these objects.

Until recently, many believed that the Cohen-Schwartz (CS) star (Cohen and Schwartz 1979) was the agent driving the HH1-2 system. This belief has been disputed by recent *VLA* radio continuum observations (Pravdo *et al.* 1985). These observations revealed a new and more viable energy source candidate for the system.

1. Present address: Instituto de Astrofísica de Andalucía, España.

This source –known as the Central Source– is located close to the center of the line connecting HH1 and HH2, and has a spectrum that is consistent with that of an ionized isothermal stellar wind ($\alpha = 0.6$, with $S_\nu \sim \nu^\alpha$). The geometrical disposition of the Central Source with respect to HH1 and HH2, as well as its spectral characteristics, are the main reasons as to why this source is now thought to be the most likely powerhouse of the HH1-2 system. No optical counterpart is seen at the position of the Central Source, this being probably due to the presence of a high density structure around the region where the source lies. In fact, an elongated structure centered at the Central Source was detected in the $(J,K) = (1,1)$ ammonia inversion transition line (sensitive to densities $n(H_2) > 5\times10^3$ cm^{-3}). This structure is seen to be aligned perpendicularly to the line connecting HH1 and HH2 (Torrelles *et al.* 1985). This alignment is very similar to those found amongst most sources with bipolar molecular outflows (Torrelles *et al.* 1983), where high density structures are perpendicular to the outflows. These structures are interpreted as toroids focussing an isotropic stellar wind in two opposite directions, in the manner described by Barral and Cantó (1981) or Königl (1982). With these sources in mind, Torrelles *et al.* (1985) concluded that the ammonia structure in HH1-2 is a toroid seen edge on, capable of producing a bipolar flow from an originally isotropic wind emerging from the Central Source. The suggestion that the Central Source is the agent driving the HH1-2 system has also been supported by infrared observations that reveal emission at the position of the Central Source, both in the near IR (Tapia, Ruiz, and Roth 1985) and at 100 μm (Harvey *et al.* 1985), and, at 2 μm, from a nearby diffuse nebula (Harvey *et al.* 1985; Rodríguez, Roth, and Tapia 1985; Strom *et al.* 1985; Tapia *et al.* 1985). Finally, polarization measurements (Warren-Smith 1985; Strom *et al.* 1985) rule out the CS star as being the energy source of the system, suggesting instead that this source is located in the region where the Central Source is.

We decided to study the HH1-2 region with the *Mepsicron* detection system in order to try to locate the optical counterpart of the Central Source, or some structural detail that might reveal any connection between this source and HH1 or HH2, as had been suggested in previous studies of the region (Mundt 1983; Wehinger 1985). Furthermore, we decided to obtain images of the region using a set of filters well suited to explore the nature of the HH1-2 system.

This paper is organized as follows. In section II we describe the instrumentation and the observations, and in section III we discuss data reduction. The images are presented in section IV and discussed in section V. Section VI is dedicated to our main conclussions.

II. THE OBSERVATIONS

The images presented in this paper –Figures 1-5 (Plates)– were obtained with the *Mepsicron* detection system (Firmani *et al.* 1982, 1984 and 1985; Bohigas 1985*a*). The detector was placed at the F/7.5 secondary focus of the 2.12-m telescope of the Observatorio Astronómico Nacional at San Pedro Mártir, Baja California, México. Interference filters with bandwidths of $\sim$ 50 A and centered at 6557, 6648 and 6734 A were used. The filter at 6557 A is almost centered at the Hα line, with some contribution from the [N II] emission lines at 6548, 6584 A (the 6584 A line is at $\sim$ 50% of the filter's peak transmission (PT) and the 6548 A line is at $\sim$ 95% of PT). Though the sum of the red [N II] lines can be comparable to Hα in HH objects (Cantó 1981), we will designate this image as the Hα image. The filter centered at 6648 A is almost free of any strong emission line, since the closest ones –[N II] at 6584 A and [S II] at 6717 A– are practically outside the filter's transmission curve (at 4% and 2% of PT). Thus, the image obtained with this filter can be regarded as a red continuum image of the field. Finally, the only emission lines likely to be present at the 6734 A filter are the [S II] lines at 6717 and 6731 A (6731 is at the filter's PT and 6717

TABLE 1

OBSERVING DATA

Image	Plate	Observation Date	Exposure Time (min)	Filter[a] λ_0 (A)	Filter[a] $\Delta\lambda$ (A)	Filter[a] Peak Transmission (PT)	Lines in the Filter
Hα	1,2	26-27, Jan.-1985	80	6557	51	75.5%	Hα at PT [N II] (6548A) at 0.95 PT [N II] (6584A) at 0.50 PT
Continuum	3	26-27, Jan.-1985	80	6648	54	70.5%	... ...
[S II]	4	27-28, Jan.-1985	80	6734	53	80.0%	[S II] (6717A) at 0.75 PT [S II] (6731A) at PT

a. λ_0 = central wavelength. $\Delta\lambda$ = bandwidth (FWHM).

is at approximately 75% of PT). The image associated to this filter will be designated as the [S II] image. The observing dates, exposure times and details on the filters used in order to obtain these images are all given in Table 1.

The *Mepsicron* is a two dimensional photon counting system. The system is made of two basic components; the detector, and an electronic device where the position and time of arrival of each event is codified (Pulse Position Analyzer or *PPA*). The detector is composed of three basic elements; a photocathode, a set of microchannel plates where the electron produced by the photocathode is amplified up to 10^8 times, and a resistive anode. The microchannel plates produce an electron cloud that falls on the resistive anode, generating electric currents that travel to each one of the four corners of the anode. From these points they are sent to the electronic peripherals in order to be amplified and analyzed. The analysis of the position and time of arrival of each event is carried out at the *PPA*. The temporal and spatial resolution of the system is set by this device, and is equal to 200 ns and 25 X 25 μm respectively. Since the diameter of the detector is approximately equal to 25 mm, this means that there are nearly 800 000 picture elements in the system. Finally, information can be stored event by event in magnetic tape, or an integrated signal can be stored in a 16 bits deep 2Mb random access memory. Some of the instrument's best qualities are its low internal noise level (only 6 X 10^{-5} counts s^{-1}-pixel^{-1} at -30 °C), its high spatial resolution (42 μm at FWHM over the whole surface), its linearity, its dynamic range (close to 10^6) and, finally, the fact that it works in a real time basis. On the other hand, the quantum efficiency of the photocathode at 4000 A is close to 24%, but it is only 3.6% at Hα, which is the spectral region where most CCD's are more effective. Thus, the *Mepsicron* system may have an advantage over the CCD's at the blue spectral region, but this superiority disappears in the red region due to poor efficiency of the photocathode. Of course, this disadvantage might be overcome with a photocathode having a superior red quantum efficiency.

The optical system used to obtain these images has a resolution of approximately 13″ mm^{-1}. Thus, the field of view of the detector is roughly equal to 5′, though the effective field is closer to 4′ due to vigneting effects occurring at the photocathode. The resolution of the detector is approximately equal to 0.35″ pixel^{-1} over the whole field. Since the seeing was rarely better than 2″ during our observing season, we decided to rebin the data in both directions to give a scale of $\sim$ 0.70″ pixel^{-1}.

III. DATA REDUCTION

Data reduction was carried out in a Prime 550-II computer working in combination with a Grinell image processing system. The images were processed with a set of software programs that have been developed at the Instituto de Astronomía of the Universidad Nacional Autónoma de México (Serrano and Ramos 1984; Barral 1985; Bohigas 1985*b*). All the original images, obtained

TABLE 2

PHOTOMETRY OF THE HH1-2 REGION

Region	Hα/Hα (HH2A) this work	Other works	[SII]/Hα this work	Other works	6648/Hα this work
HH1F	0.69	0.92	0.29	0.30	0.05
HH2A	1.0	1.0	0.15	0.15	0.04
HH2B	0.18	0.13	0.35	0.37	0.06
HH2C	0.17	0.08	0.47	0.52	0.06
HH2D	0.17	0.09	0.48	0.68	0.11
HH2E	0.06	0.07	0.84	1.43	0.07
HH2G	0.25	0.22	0.29	0.40	0.06
HH2H	0.78	0.65	0.20	0.19	0.05
Sulphur Condensation	0.02		1.14	0.94[a]	0.03
Western Arch	$\sim$ 0.02		$\sim$ 0.35		$\sim$ 0.10
Sulphur Filaments	0.02		0.85		0.05
Western HH Objects	0.01		0.32 – 0.70		

Data from other works is from Hartmann and Raymond (1984), except for (a), which is from Cohen and Fuller (1985). Measurements from other works were transformed taking into account the contribution of each emission line in each filter. Our measurements were carried out with a circular 3″ diaphragm. Relative intensities in the Hα image are with respect to HH2A, and given as Hα/Hα(HH2A).

as indicated in Table 1, were divided by a normalized flat field. Beyond this, each image was processed as described below.

a) *Hα Image*

A mean sky background, estimated at 212 counts per pixel, was subtracted from the flat fielded Hα image. The resulting image was passed through median filters with different sized windows. Figure 1 (Plate) was obtained with a 5 X 3 pixel window, whereas in Figure 2 (Plate) we used a 10 X 10 pixel window. Such a filter has the virtue of removing the high frequency noise and increasing the image contrast, but at the price of a degraded spatial resolution. In order to display the faintest structures in the field, the number of counts in the brightest regions (HH1 and HH2) was artificially reduced. Thus, the contrast between the brightest features and the mean level, as it appears in Figures 1 and 2 (Plates), is not linear. The real contrast is approximately equal to 30 to 1. A reflection (to be discussed in §IV), which is particularly intense in the continuum image (see Figure 3, Plate), appeared to the north of the field. This reflection is localized in a rather narrow band where few important features are present, so that it was possible to subtract the continuum image from the Hα image in order to perform photometric measurements over most of the field. The two images were calibrated with the CS star, in which the ratio of Hα to the nearby continuum emission over a 50 A wavelength range (equal to the filters' bandwidths) is between 0.3 and 0.5 (Cohen and Schwartz 1979; Mundt and Hartmann 1983). Thus, the continuum and Hα images were matched so as to have this ratio at the CS star. The matching was checked with the ratio of the continuum and Hα emission measurements carried out by Brugel, Böhm, and Mannery (1981*a* and 1981*b*), in condensations HH2A, HH2G and HH2H. Discrepancies with these ratios are within the error bars of their continuum measurements (i.e., within a factor of 2-3). We also made an inquest into the relative Hα intensity over several condensations in the field, using the spectroscopic observations made by Hartmann and Raymond (1984) in order to assess our results. Their measurements were corrected taking into account the contribution of each emission line in each filter, and they are displayed in Table 2, where our photometric results are shown. Relative Hα intensities in most condensations are well within a factor of 2 from those determined by Hartmann and Raymond (1984). As they estimate that their measurements are accurate within a factor of 2, we regard our results as coincident with theirs. This precision is maintained in weaker signals, for the *Mepsicron* system is linear (linearity has been confirmed with direct images of M15 over the observed magnitude range, i.e., from $m_V = 14.3$ to $m_V = 19.2$). Finally, the continuum image has not been subtracted from the Hα image in Figures 1 and 2 (Plates). as the strong continuum reflection is awkwardly distracting. In spite of this omission, we believe that Figures 1 and 2 accurately represent the distribution of Hα and [N II] emission over the whole field, since the continuum underlying the Hα image is never more than 10-20% of the line emission (see Table 2 and Figure 7).

b) *Continuum Image*

The number of counts in the brightest regions of the continuum image (Figure 3, Plate) was also artificially reduced. We decided not to subtract the sky background or pass a median filter through this image, so as not to loose the faint and thin filamentary structures that appear in Figure 3 (Plate) (see §IV). The subtraction of the sky level results in the fragmentation of these filaments, whereas a median filter washes them out in the general background. On the other hand, photometric measurements were carried out once we subtracted a sky level of 68 counts per pixel from the continuum image.

c) [*S II*] *Image*

The [S II] image –Figure 4 (Plate)– was obtained in the same manner as the Hα image. In this case the sky background was estimated to be at 189 counts per pixel, and the median filter applied to this image had a 5 X 3 pixel window. The real contrast between the brightest features and the mean level is roughly equal to 10 to 1. In order to perform photometric measurements, the continuum image was subtracted from the [S II] image, using once more spectroscopic observations carried out at the CS star (Cohen and Schwartz 1979; Mundt and Hartmann 1983) in order to calibrate both images. Finally, continuum emission has not been subtracted from the [S II] image in Figure 4 (Plate), because of the annoying reflection appearing in the continuum image. As sulphur emission is at least $\sim$ 3-4 times larger than the continuum underlying the [S II] image over most of the northern and southern cones (see Figure 7), we think that Figure 4 (Plate) is a reasonably close representation of the overall distribution of the emission from the red [S II] lines in the HH1-2 region.

d) *Image of the* [*S II*] *to Hα Ratio*

This image –Figure 5 (Plate)– was obtained from the flat fielded images of Hα and [S II], from which their respective sky background was subtracted. The two images were repositioned using the CS star before taking the ratio, which was calculated at each pixel. Any value larger than 2.5 or less than 0.1 was made to be zero. These are reasonable limits for any kind of nebula (Sabbadin and D'Odorico 1976). A median filter with a 3 X 3 pixel window was applied to the resulting image. Again, photometric measurements were performed once we subtracted the continuum image from the [S II] and Hα images (all of them without the sky background). Our results appear in Table 2, where we also included measurements made by other authors (Hartmann and Raymond 1984; Cohen and Fuller 1985). The latter

were corrected taking into account the contribution of each line in each filter. With the exception of HH2E, our ratios agree with their results within 30%, in objects as bright as HH2A or as faint as the sulphur condensation (see below). Though the Hα image contains information on the red [N II] lines, from now on we will refer to any value in the image of the ratio of the [S II] to Hα images, as [S II]/Hα.

IV. IMAGE DESCRIPTION

There are several salient features (schematically represented in Figure 6) in the images obtained for the region around HH1 and HH2. Not all of them appear in all images, and therefore these are discussed separately.

a) *Hα Image*

The overall Hα properties of the region are probably more apparent in Figure 2 (Plate), where information on the gross details of the field is enhanced. The image was contaminated by a reflection due to the star V380 Ori, which is $\sim 3'$ NE away from HH1 and outside the field of view. The reflection was not detected on time because a series of short 10 minute exposures were made since the auto-guiding system was not in operation. The reflection became stronger as the observations proceeded, until it was very noticeable in the continuum image (see Figure 3, Plate). The reflection is more pronounced at the northern edge of the field, becoming weaker at the field center, where it contributes with ~ 10 counts per pixel in the Hα image.

The overall Hα distribution is quite striking. There is an obvious depression in Hα emission in the NE–SW direction, which is, not surprisingly, the region at which the dense disk-like ammonia structure was detected by Torrelles *et al.* (1985). This emission 'void' is nearly perpendicular to the line connecting HH1, the Central Source and HH2.

Other interesting features are the two arches that seem to protrude from the northern tip of HH2. The western arch is quite bright, and it appears in a number of plates of the region (Herbig and Jones 1981; Wehinger 1985). The eastern arch is considerably fainter. It has a mean value of 36 counts per pixel over the sky level, as opposed to 66 counts per pixel in the western arch, but it is definitely above the sky level ($\sim 7\sigma$, where σ is the standard error of the mean). Its existence can be guessed in the image of the region obtained by Wehinger (1985). The symmetric disposition of these two arches is somewhat mistyfying, and it may well be just a coincidence designed to puzzle the theorist.

A third, and very important feature in this image, is a structure arising from the western arch and directed towards the region at which the Central Source is located. This structure is also relatively weak (at $\sim 6\sigma$ over the sky level), but we think that it is real as it is also seen in the [S II] image. It is interesting to notice that no significant emission was detected at the position of the Central Source, whose location was determined with an offset from the CS star, and verified with other field stars.

An emission bridge (henceforth the northern cone) connecting the Central Source to HH1 is also evident. This has also been observed by Herbig and Jones 1981, Mundt (1983), Strom *et al.* (1985) and Wehinger (1985), but it is important to notice that it has a relatively sharp western edge (see Figure 2, Plate), as opposed to the rather smooth emission decay that can be seen on its eastern side.

Emission can also be seen to extend to the east of HH1, connecting this source to a number of condensations that are also seen in the Plates taken by Herbig and Jones (1981) and Wehinger (1985). Finally, there seems to be a northeastern emission ridge between these condensations and the Central Source, so that a cavity is apparently defined in the northern region of the field. Unfortunately, the existence of the northeastern emission ridge (hence, of the cavity) is somewhat doubtful, as it lies at the position where the reflection produced by V380 Ori is. At present, we cannot conclude if there is any intrinsical Hα emission from the HH1-2 region under this reflection.

b) *Continuum Image*

The maximum continuum emission is reached at the position of knot A in HH2, with 209 counts per pixel, 21 times less than the number of counts per pixel for the same knot in the Hα image. The observed sky level is at 68±2 counts per pixel. The obnoxious reflection that appeared in the Hα image is now painfully evident. This reflection becomes weaker towards the field center, but in this case it has an important effect on the region where the Central Source is.

None of the large structural elements that could be seen in the Hα image, such as the emission depression in the NE–SW direction and the connection between the Central Source and HH1 or HH2, are clearly visible in Figure 3 (Plate). On the other hand, two very delicate filamentary structures jut out in the continuum image. The first of these extends from the CS star to a point close to the position where the Central Source is. It has a PA of $\sim 130°$ near the CS star. The second filament is associated to HH2 and directed towards the region where the Central Source is. The signal to noise ratio in these filaments is $\sim 6\sigma$, and we estimate that they are $\sim 5''$ wide.

c) [*S II*] *Image*

In order to avoid the unpleasant reflection caused by V380 Ori in the Hα and continuum images, we displaced the field center $\sim 0.6'$ to the SW. Fortune was not at hand during our observing run, and we managed to get a different reflection in the [S II] image (Figure 4, Plate). This was due to moonlight, and it appears in the SW di-

rection. This reflection has a relatively small effect on the central region, where we estimate that it is at $\sim$ 16 counts per pixel over the sky level. The sky level is at 189±3 counts per pixel, and the maximum intensity is reached in knot A in HH2, with 866 counts per pixel (compared to 4348 counts per pixel at the same position in the Hα image).

A remarkable property of the [S II] image is the likeness between its overall structure and that of the Hα image. Several important features of the latter are also clearly visible in sulphur emission. A western arch can be seen to rise from HH2 both in Hα and in the red [S II] lines (notice that the eastern arch cannot be seen in the [S II] image since the field center was displaced), and the northern cone is very bright in both images. A second structure, associated to HH2 and directed towards the Central Source (the southern cone), in contrast to the Hα image, is very well defined in the [S II] lines. Also important is the emission between the western arch and the Central Source, which is particularly conspicuous in the [S II] image, where a second connection reaching towards the Central Source, $\sim$ 25″ to the E of the first one, can also be barely distinguished from the general background ($\sim 6\sigma$). On the other hand, the dramatic NE–SW emission defficiency found in Hα, is not nearly as evident in the [S II] image. This can be due to the fact that the center of this image is displaced with respect to the center of the HH1-2 field.

But the [S II] image reveals many more small structure details than the hydrogen image. This indicates that sulphur emission, even if it has the same general outline as the Hα emission, is more concentrated, and does not pervade the whole HH1-2 region, as hydrogen emission seems to do. No sulphur emission is seen in the region where the Central Source is. This region seems to be wrapped by an almost complete circle of sulphur emission, but the reality of this small and suggestive envelope is very uncertain. Some 10″ NW of the Central Source there is an intense nebulosity (90 counts per pixel over the sky level), which is confused with the general background of the Hα emission, and is almost absent in the continuum image. This nebulosity (henceforth the 'sulphur nebulosity') is at the position of the near-IR source discovered by Rodríguez, Roth, and Tapia (1985). Its nature and relevance will be discussed in the next section. About 20″ to the W of the Central Source there are two knots (at $\sim 7\sigma$) which were also detected through CCD images (Strom *et al.* 1985). Again, as in the case of the sulphur nebulosity, these knots are very clearly brought out in the [S II] image. They are almost lost in the general background of the Hα image, and are practically invisible in the continuum

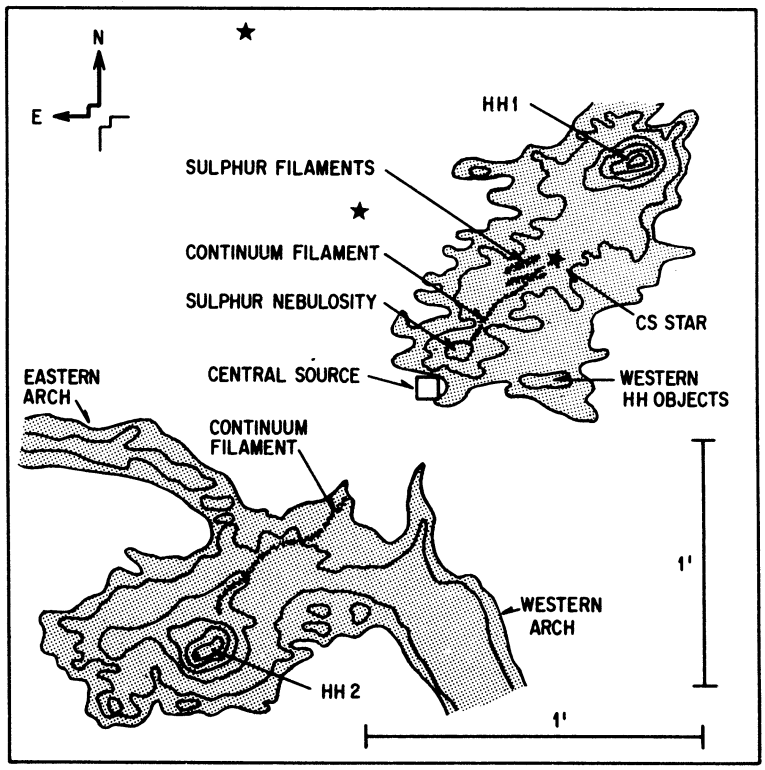

Fig. 6. Schematic representation of the most interesting features in the HH1-2 region. This figure is a composite of the Hα, continuum and [S II] images. The relative brightness of the continuum and sulphur filaments has been artificially enhanced.

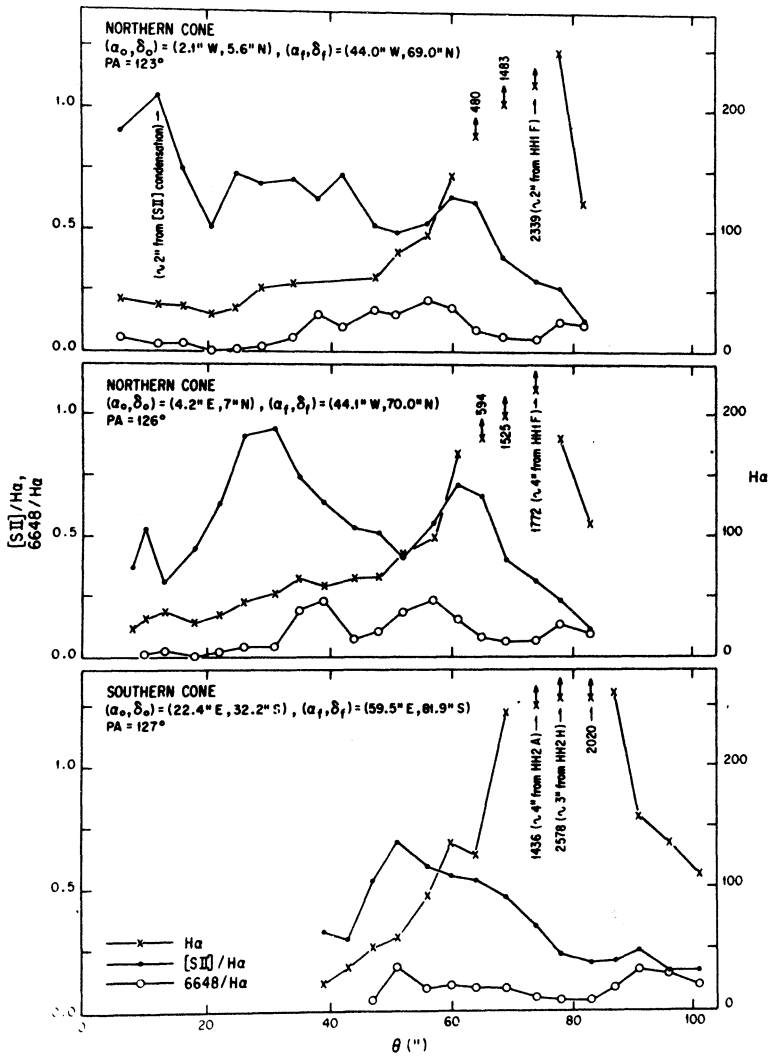

Fig. 7. Scans along the northern and southern cones. Measurements were made with a circular 5" diaphragm. Positions (θ) are relative to the Central Source, and we estimate them to be accurate within 2". The positions of the two extreme positions of each scan are given as (α_0, δ_0) and (α_f, δ_f), and are also measured with respect to the Central Source. The ratio of continuum to Hα emission is indicated as 6648/Hα, whereas Hα is given in number of counts per pixel. The diaphragm contains 29 pixels.

image. Finally, the [S II] image reveals two nearly parallel filaments close to the CS star with a PA of $\sim 120°$ (henceforth the 'sulphur filaments'). These are $\sim$ 3-4" wide, and are separated by $\sim$ 4". They are definitely over the sky level (at $\sim 20\sigma$), and the similar PA and spatial position of the continuum filament near the CS star insinuates that the same feature is being observed in both images A discussion on these filaments will be given in the next section.

V. DISCUSSION

The images presented in the previous section reveal several interesting properties of the HH1-2 region. An important result is the overall structure as seen in the Hα image (Figures 1 and 2, Plates), and in particular the lack of Hα emission along the high density ammonia structure, supporting the idea that a molecular disk is collimating a stellar wind in two opposite directions. Furthermore, the presence of two conical structures connecting HH1 and HH2 to the Central Source, in the [S II] image as well as the Hα image, suggests that the latter is the energy source of the system, and not the CS star, which is far from the center of symmetry of the system and is not connected to HH2.

One of the most interesting results is the large difference of the Hα and [S II] images with respect to the continuum image. In the first two images (Figs. 1, 2 and 4 , Plates), the conical structures connecting HH1 and HH2 to the Central Source are clearly delineated. This does not occur in the continuum image, where these structures are marginally detected as they are

lost in the general background. This difference is quantified in Figure 7, where we plot a set of scans along the northern and southern cones. Figure 7 reveals that the ratio of continuum to Hα emission (6648/Hα) is far from uniform, and on the average equal to 0.09. It is about half this value in the brightest condensations (HH1F, HH2A and HH2H), and it can be as large as 0.23 in a couple of positions along the northern cone. The variations and values taken by this ratio, suggest that line emission in the two conical structures is essentially produced *in situ*. On the other hand, the continuum is probably produced by reflected light, since the ratio of continuum to Hα emission in a thermal plasma is $\sim$ 1/100, much less than what is revealed by the set of scans carried out along the two cones. The latter conclusion is in agreement with the high degree of polarization observed in the two conical structures (Warren-Smith 1985; Strom *et al.* 1985), which indicates that there is a component of reflected light in both nebulae. However, the polarization observations cannot be interpreted as evidence for a model in which all light arising from the HH1-2 region is reflection from a point source, as these observations were carried out with a broad-band filter (I) with which continuum emission is bound to dominate line emission. To prove the latter it would be necessary to carry out line polarization measurements, or to compare line images with continuum images obtained with narrow-band filters where no emission lines are transmitted, as has been done in this paper. Our conclusion in this respect is clear; the difference of the continuum image with respect to the Hα and [S II] images, as well as the variations in the continuum to Hα ratio and the complex structure revealed in the [S II]/Hα image, indicate that line emission is produced *in situ* and is not reflected.

In a collisionally ionized nebula, such as Herbig-Haro objects, the line ratio Hα/([S II] = 6717+6731 A) is typically less than 2.5 (Sabbadin and D'Odorico 1976; Sabbadin, Minnello and Bianchini 1977; Cantó 1981). Thus, the image of the sulphur to hydrogen ratio (Figure 5, Plate) can provide information as to the exciting mechanism in any zone of the HH1-2 region. Estimating the contribution of each line in the Hα and [S II] images, we find that any value larger than $\sim$ 0.3 in the image for [S II]/Hα indicates collisional ionization. An analysis of this image (see Figure 7) reveals that, for the most part, the conical structures connecting HH1 and HH2 to the Central Source are collisionally ionized, though there are some regions where the ratio is close to 0.2. It is interesting to notice that some of these regions are amongst the brightest in the field (for instance, knots A and H in HH2), which indicates a high density in them. If so, collisional de-excitation of the [S II] lines in these regions can be of some importance, and the value of [S II]/Hα in the collisionally excited gas will be smaller than what is normally seen. As a matter of fact, Hartmann and Raymond (1984) carried out spectroscopic observations of these knots, and concluded that the small values of [S II]/Hα can be explained in terms of a bow shock moving into a dense medium ($n = 100$ cm^{-3}). The behavior of [S II]/Hα, which is shown in Figure 7, also supports the idea that line emission in the northern and southern cones is produced *in situ*, and is not reflected light. First, because the ratio is far from being uniform. Secondly, the relatively high intensity of the sulphur lines in comparison to Hα is difficult to explain in terms of light reflected from a young stellar object, as these are not generally characterized by having strong [S II] emission.

Several local features merit some discussion. The highest [S II]/Hα ratio ($\sim$ 1.15) is found in the sulphur condensation, which indicates that this region is excited by a shock wave. Recent spectroscopic observations of the region (Cohen and Fuller 1985) confirm this, showing that this condensation is probably another Herbig-Haro object. An intriguing feature in the field is the apparent identity between the continuum filament that extends from the CS star to the Central Source, and the sulphur filaments. A careful study of their positions reveals that they have slightly different orientations, and are not located in the same region. The continuum filament is roughly located at the center of the conical structure that extends from the Central Source to HH1. The complement of this filament can be the other continuum filament going from the Central Source to HH2, and located at the center of the southern cone. Thus, we think that the continuum filaments delineate the apex of the two conical structures. On the other hand, the sulphur filaments are probably shock heated, since [S II]/Hα $\sim$ 0.85 in them. Consequently, it is tempting to assume that these two filaments are 'jets' emerging from the CS star, a phenomenon that may be occurring in other regions (Mundt, Stocke,and Stockman 1983). Yet, their disposition with respect to the CS star suggests that this is probably not the case, as these filaments do not emerge from the CS star, but pass $\sim 2''$ away from it. Hence, they are probably part of the general emission of the northern cone, and their appearance can be explained in terms of projection and extinction effects (Cantó, Sarmiento, and Rodríguez 1985). As mentioned in §IV, $20''$ and $24''$ to the W of the Central Source there are two emission knots that are very conspicuous in the [S II] image. The [S II]/Hα ratio at their position is 0.32 and 0.7 respectively, which indicates that these knots are collisionally ionized, and quite possibly HH objects (Strom *et al.* 1985). The value of this ratio in the emission bridge between HH2 and the Central Source, as well as in the western arch emerging from HH2, is $\sim$ 0.3-0.4. This suggests that both structures are collisionally ionized, though further studies are required in order to clarify their nature. Finally, as we do not detect optical emission from the Central Source, we estimate a limiting magnitude of V $\sim$ 21.5 for this object.

VI. CONCLUSIONS

Images of the HH1-2 region with the *Mepsicron* system were obtained with filters centered at 6557 (Hα image), 6648 (continuum image) and 6734 ([S II] image) A. These images revealed a complex structure in the region, with several salient features. Our main conclusions can be summarized as follows:

i) We detected two conical structures connecting the region around the Central Source to HH1 and HH2. No prominent optical emission was observed along the region perpendicular to the line defined by HH1, the Central Source and HH2. The region where optical emission is absent, coincides with the elongated ammonia structure found previously.

ii) The [S II] image reveals a prominent nebulosity $\sim 10''$ NE of the Central Source. This nebulosity (the sulphur nebulosity) is at the position where an extended near-infrared source was discovered. This image also reveals a couple of knots $\sim 20''$ W of the Central Source.

iii) The Hα image presents two remarkable arch-like features that seem to emerge from HH2. These arches are located to the E and W of HH2, and have a symmetric disposition with respect to the latter.

iv) None of the previous features are conspicuous in the continuum image. This difference, added to the large values and complex structure found in the image of the ratio of the [S II] to Hα images, indicates that the emission lines are produced *in situ*. On the other hand, a comparison between Hα and continuum emission, indicates that the continuum is mainly reflected light, possibly from the Central Source, and not free-free emission produced *in situ*. This last conclusion is supported by polarimetric measurements of the continuum carried out by other authors.

v) The image of the ratio of the [S II] to Hα images indicates that emission in the structures described above is consistent with a collisional ionization mechanism. Thus, we think that the sulphur nebulosity and the two knots located $\sim 20''$ W of the Central Source, are probably HH objects. Furthermore, we propose that the two conical structures were created, and are collisionally excited, by the stellar wind of the Central Source, which is probably collimated by the high density ammonia cloud.

vi) We did not detect optical emission at the position of the Central Source. This implies a limiting visual magnitude of ~ 21.5 for this object.

vii) These are the first reported images obtained with the *Mepsicron* system. The system's performance has proved to be highly satisfactory, and future work with the system is likely to produce new and interesting astronomical results.

We would like to thank M. Shara for kindly letting us use his filters during our observing season, S. Strom for a very positive criticism, and A. García for his drawing work. This is Contribution No. 185 of Instituto de Astronomía, UNAM.

REFERENCES

Barral, J.F. 1985, *Technical Report No. 23*, Instituto de Astronomía, UNAM, México.
Barral, J.F. and Cantó, J. 1981, *Rev. Mexicana Astron. Astrof.*, **5**, 101.
Bohigas, J. 1985*a*, *Technical Report No. 19*, Instituto de Astronomía, UNAM, México.
Bohigas, J. 1985*b*, in preparation.
Brugel, E.W., Böhm, K.H., and Mannery, E. 1981*a*, *Ap. J.*, **243**, 874.
Brugel, E.W., Böhm, K.H., and Mannery, E. 1981*b*, *Ap. J. Suppl.*, **47**, 117.
Cantó, J. 1981, in *Investigating the Universe*, ed. F.D. Kahn (Dordrecht: D. Reidel), p. 95.
Cantó, J., Sarmiento, A., and Rodríguez, L.F. 1985, in preparation.
Cohen, M. and Fuller, G.A. 1985, preprint.
Cohen, M. and Schwartz, R.D. 1979, *Ap. J. (Letters)*, **233**, L77.
Firmani, C., Ruiz, E., Carlson, C.W., Lampton, M., and Paresce, F. 1982, *Rev. Sci. Instrum.*, **53**, 570.
Firmani, C. *et al.* 1984, *Astr. and Ap.*, **134**, 251.
Firmani, C., Ruiz, E., Bohigas, J., and Bisiacchi, G.F. 1985, *Rev. Mexicana Astron. Astrof.*, in press.
Haro, G. 1950, private communication of May 31 to Drs. H. Shapley and R. Minkowski.
Haro, G. 1952, *Ap. J.*, **115**, 572.
Hartmann, L. and Raymond, J.C. 1984, *Ap. J.*, **276**, 560.
Harvey, P.M., Joy, M., Lester, D.F., and Wilking, B.A. 1985, *Ap. J. (Letters)*, in press.
Herbig, G.H. 1951, *Ap. J.*, **113**, 697.
Herbig, G.H. and Jones, B.F. 1981, *A.J.*, **86**, 1232.
Königl, A. 1982, *Ap. J.*, **261**, 115.
Mundt, R. 1983, *Rev. Mexicana Astron. Astrof.*, 7, 53.
Mundt, R., Stocke, J., and Stockman, H.J. 1983, *Ap. J. (Letters)*, **265**, L71.
Mundt, R. and Hartmann, L. 1983, *Ap. J.*, **268**, 766.
Pravdo, S.H. *et al.* 1985, *Ap. J. (Letters)*, **293**, L35.
Rodríguez, L.F., Roth, M., and Tapia, M. 1985, *M.N.R.A.S.*, **214**, 9P.
Sabbadin, F. and D'Odorico, S. 1976, *Astr. and Ap.*, **49**, 119.
Sabbadin, F., Minello, S., and Bianchini, A. 1977, *Astr. and Ap.*, **60**, 147.
Schwartz, R.D. 1983, *Ann. Rev. Astr. and Ap.*, **21**, 209.
Serrano, A. and Ramos, M.P. 1984, *Technical Report No. 16*, Instituto de Astronomía, UNAM, México.
Strom, S.E. *et al.* 1985, *Ap. J.*, in press.
Tapia, M., Ruíz, M.T., and Roth, M. 1985, in preparation.
Torrelles, J.M., Cantó, J., Rodríguez, L.F., Ho, P.T.P., and Moran, J.M. 1985, *Ap. J. (Letters)*, **294**, L117.
Torrelles, J.M. *et al.* 1983, *Ap. J.*, **274**, 214.
Warren-Smith, R. 1985, in preparation.
Wehinger, P. 1985, private communication.

J. Bohigas, J. Cantó, R. Enríquez, C. Firmani, L. Gutiérrez, E. Ruiz, and L. Salas: Instituto de Astronomía, UNAM, Apartado Postal 70-264, 04510, México, D.F., México.
J. Echevarría: Instituto de Astronomía, UNAM, Apartado Postal 877, 22830 Ensenada, B.C., México.
J.M. Torrelles: Instituto de Astrofísica de Andalucía, Apartado Postal 2144, Granada 18080, Spain.

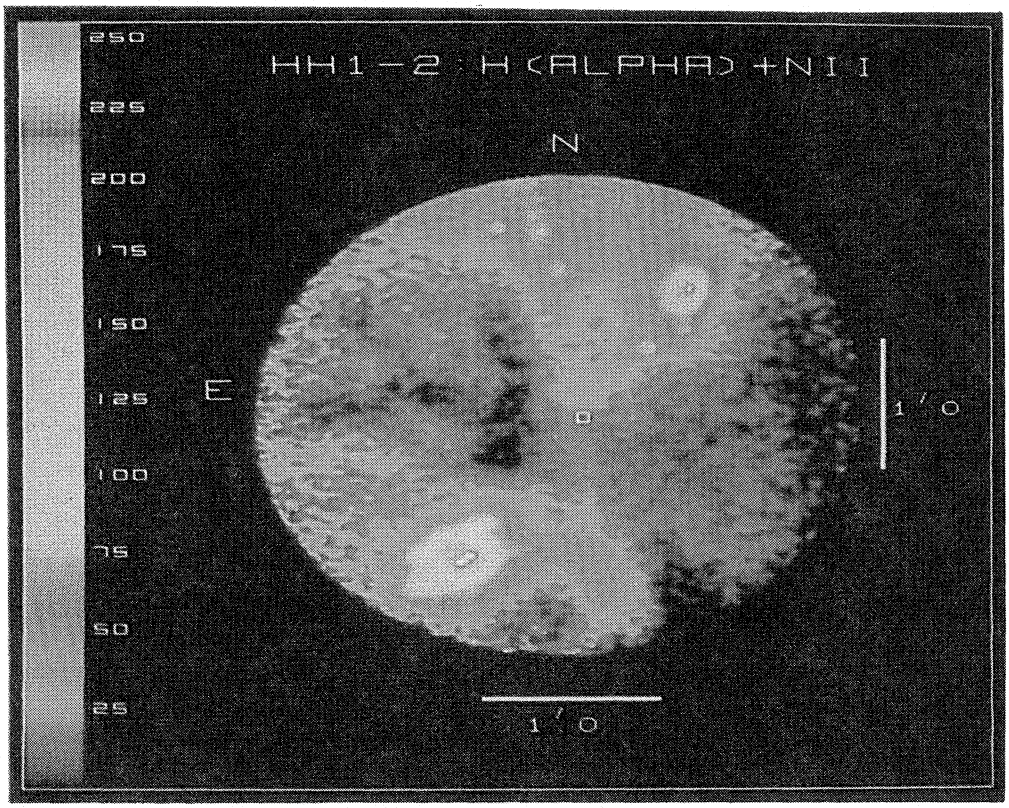

Fig. 1. Image of the HH1-2 region obtained with a filter centered at 6557 A and a 51 A bandwidth. The position of the Central Source was determined with an offset from the CS star, and verified with other field stars. It is indicated with a square in this figure, as well as in all others. A median filter with a 5 × 3 pixel window was applied to this image.

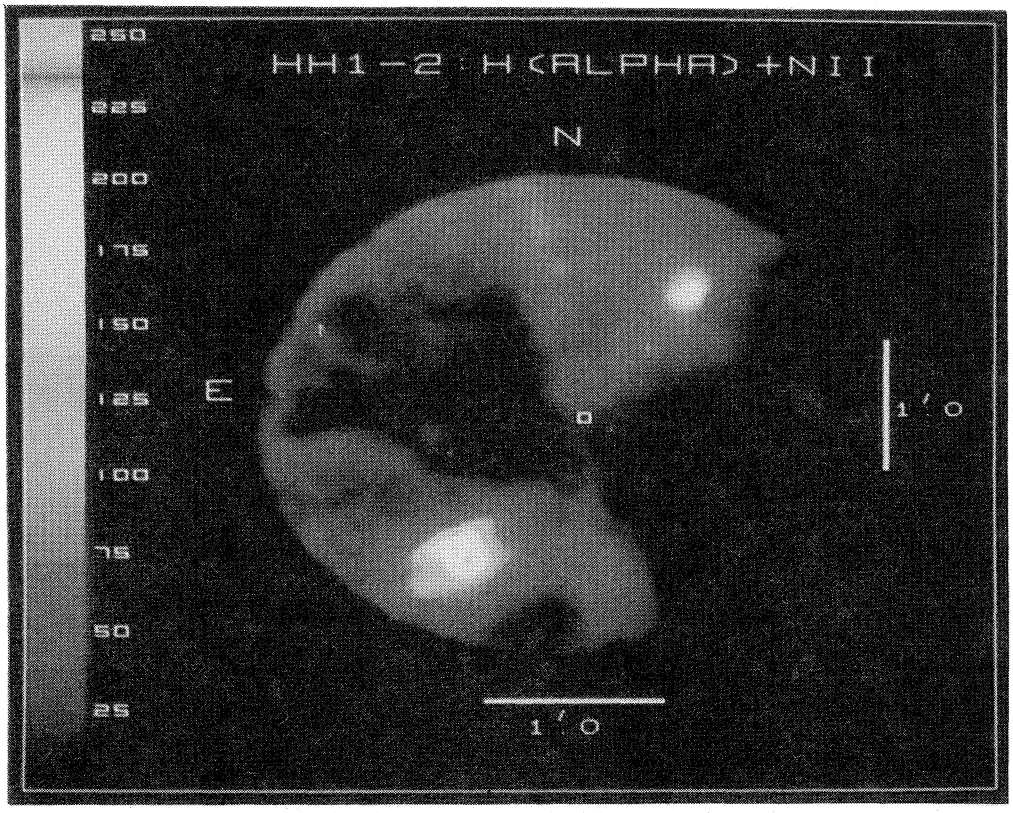

Fig. 2. Same as in Figure 1, but obtained with a median filter with a 10 × 10 pixel window.

J. BOHIGAS (See page 149)

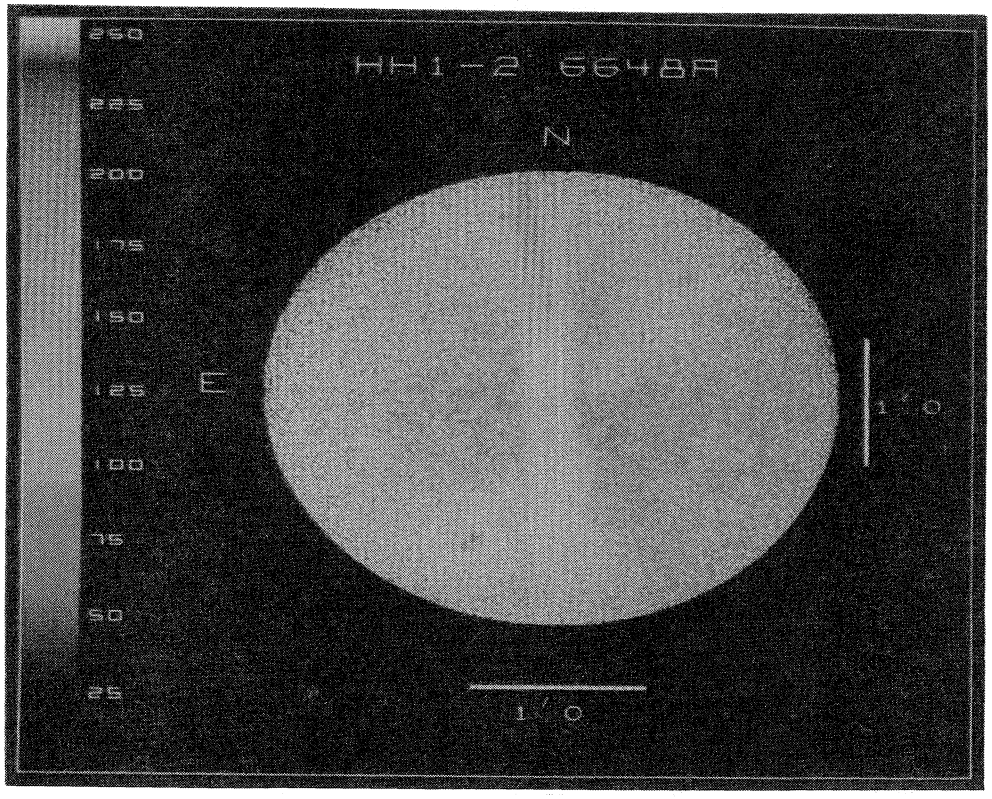

Fig. 3. Image of the HH1-2 region obtained with a filter centered at 6648 A and a 54 A bandwidth.

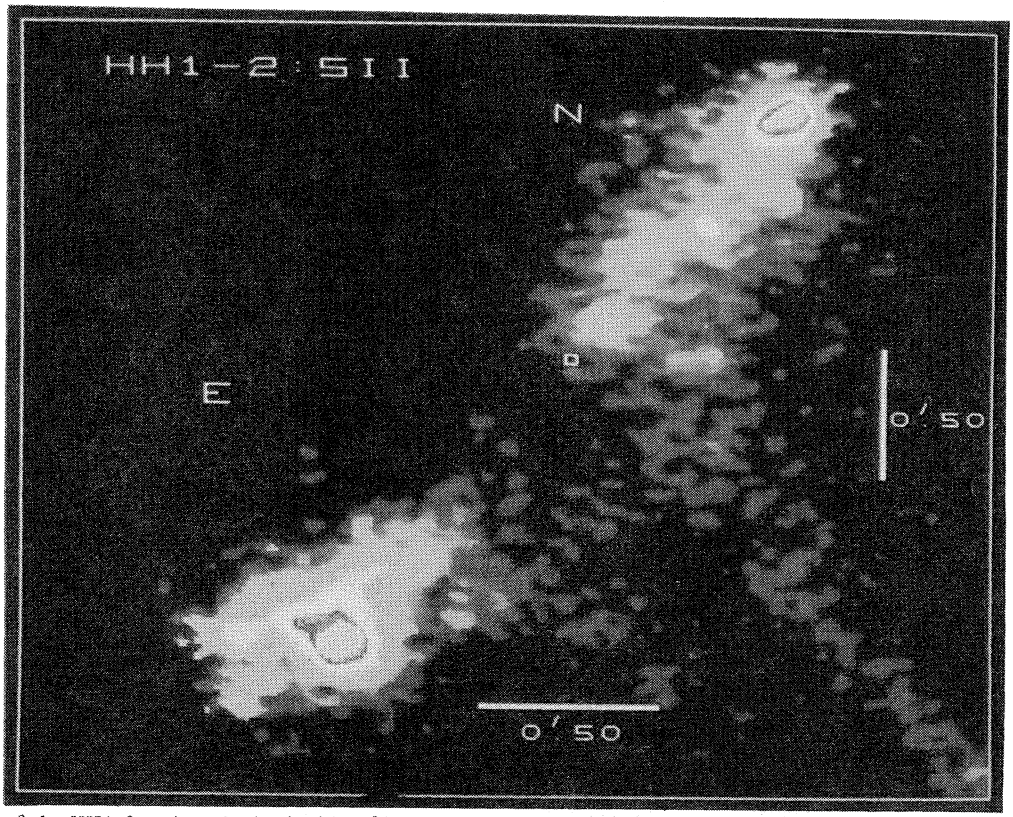

Fig. 4. Image of the HH1-2 region obtained with a filter centered at 6734 A and a 53 A bandwidth. The color scale is as given in Figure 1.

J. BOHIGAS (See page 149)

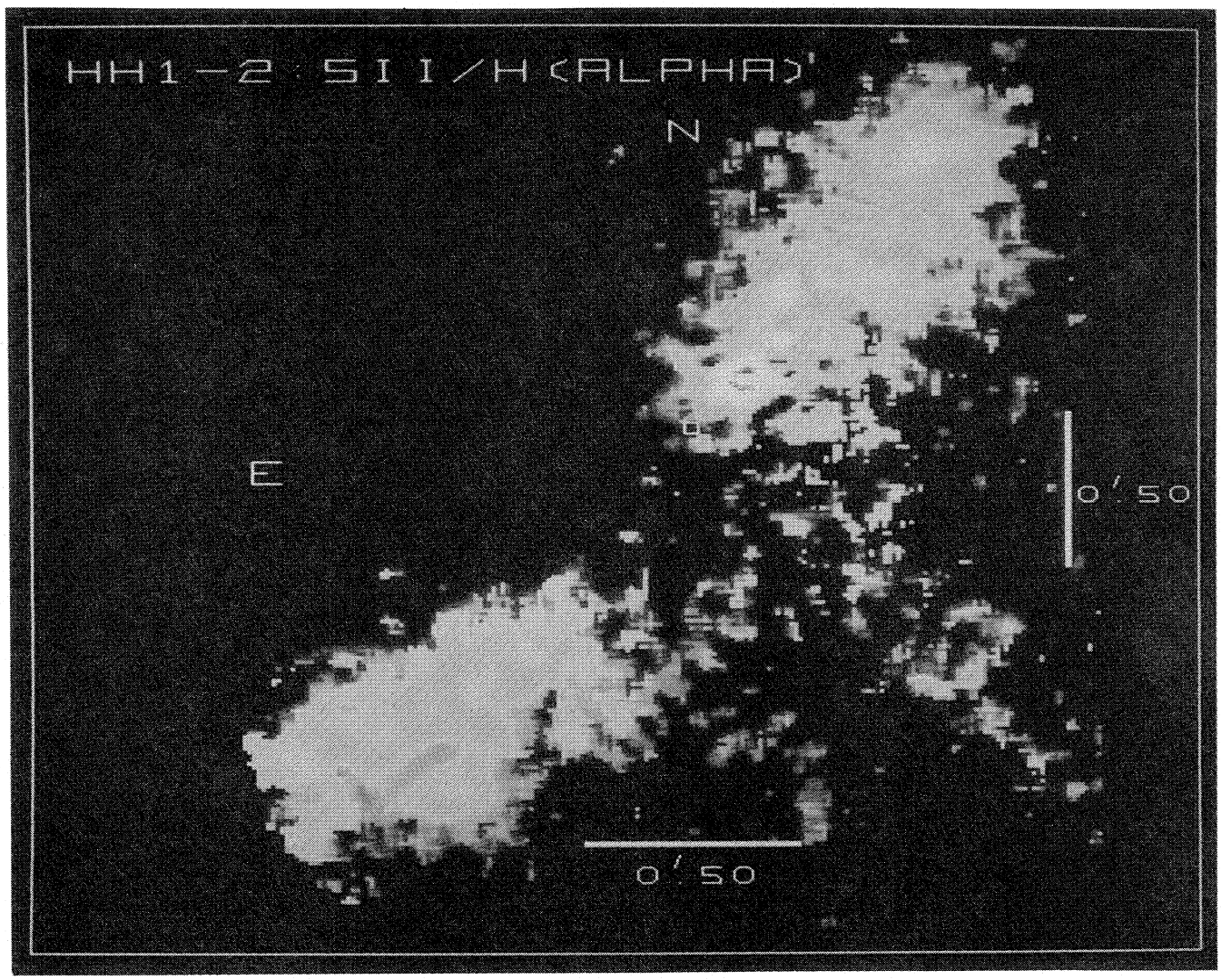

Fig. 5. Image of the ratio of the [S II] to Hα images. The ratios were multiplied by 100 in order to display the same color scale as in Figure 1.